Science of the Total Environment, Volume 630, 15 July 2018, Pages 62-71
DOI: 10.1016/j.scitotenv.2018.02.169

EXPERIMENTAL AND SIMULATION STUDY OF THE RESTORATİON OF A THALLİUM (I)-CONTAMİNATED AQUİFER BY PERMEABLE ADSORPTİVE BARRİERS (PABs)

Santonastaso G. F. [1], Erto A.[2]*, Bortone I.[3], Chianese S.[1], Di Nardo A.[1], Musmarra D.[1]

[1]Dipartimento di Ingegneria Civile, Design, Edilizia e Ambiente, Università della Campania Luigi Vanvitelli, via Roma, 29 - 81031, Aversa (CE), Italy

[2]Dipartimento di Ingegneria Chimica, dei Materiali e della Produzione Industriale, Università di Napoli Federico II, P.le Tecchio, 80 - 80125 Napoli, Italy

[3] School of Water, Energy and Environment, Cranfield University, Cranfield, MK43 0AL, UK

Abstract

Permeable Adsorptive Barriers (PABs), filled with a commercial activated carbon, are tested as a technique for the remediation of a thallium (I)-contaminated aquifer located in the south of Italy. Thallium adsorption capacity of the activated carbon is experimentally determined through dedicated laboratory tests, allowing to obtain the main modelling parameters to describe the adsorption phenomena within the barrier. A 2D numerical model, solved by using a finite element approach via COMSOL Multi-physics®, is used to simulate the contaminant transport within the aquifer and for the PAB design. Investigations are carried out on an innovative barrier configuration, called Discontinuous Permeable Adsorptive Barrier (PAB-D). In addition, an

* Corresponding author. Tel.:+39 081 7682236 Fax +39 081 5936936

E-mail address: aleserto@unina.it (A. Erto)

optimization procedure is followed to determine the optimum PAB-D parameters, and to evaluate the total costs of the intervention. A PAB-D made by an array of wells having a diameter of 1.5 m and spaced at a distance of 4 m from each other, is shown to be the most cost-effective of those tested, and ensures the aquifer restoration within 80 years. The simulation outcomes demonstrate that the designed PAB-D is an effective tool for the remediation of the aquifer under analysis, since the contaminant concentration downstream of the barrier is below the regulatory limit for groundwater, also accounting for possible desorption phenomena. Finally, the best PAB-D configuration is compared with a continuous barrier (PAB-C), resulting in a 32% saving of adsorbing material volume, and 36% of the overall costs for the PAB-D.

Keywords: Permeable Reactive Barriers (PRB); Adsorption; Groundwater remediation; Thallium; Aquifer contamination.

1. Introduction

Thallium (Tl) is an extremely toxic heavy metal. Although it is far less studied than other substances, the risk related to accidental exposure to thallium is comparable to the well-known ailments from exposure to lead and mercury (Viraraghavan and Srinivasan, 2011). It is naturally present in the earth's crust included in minerals such as sulphides (e.g. pyrite and sphalerite), feldspars and micas, where it is frequently present as a substitute of potassium (Nriagu, 1998). In the last years the diffusion of the use of Tl in high-technology applications, such as photocell, electronics and semiconductor production, has significantly increased and a further enlargement of its fields of application is expected in the future (Viraraghavan and Srinivasan, 2011). However, at present, it is believed that the major causes of Tl release to the environment are those industrial processes where Tl is present as impurity in raw materials, hence the spectrum of potential sources is quite large. The main anthropogenic sources of release of Tl to the environment are gaseous emissions and solid waste discharge, mainly arising from cement manufacture, coal and oil

combustion, non-ferrous metal mining and smelting (López Antón et al., 2013). The contamination of water bodies can occur through different pathways, including direct wastewater discharge and leaching of contaminated solid wastes, natural rocks and soils (Peter and Viraraghavan, 2005).
As a dangerous classified substance (Directive 67/548/EEC), Tl is subject to strict regulations concerning the highest admissible concentration in water. In Italy, the concentration limit for groundwater is 2 μg L^{-1}, which is the same established in the USA by the Environmental Protection Agency (U.S. EPA, 2017).
Currently, groundwater remediation technologies can be classified as *ex-situ* and *in-situ* depending on whether the contaminated water is pumped to surface or not for its decontamination (Bortone et al., 2013a). Among the *in-situ* treatments, over the past few years, permeable reactive barrier (PRB) technology has gained great consideration for its undoubted technical and economic advantages (Gavaskar et al., 2000; Obiri-Nyarko et al., 2014). Regardless of its filling material, a PRB is a trench installed into the aquifer and designed to intercept a contaminated plume flowing under the natural gradient to capture/transform the contaminant into an environmentally acceptable form (U.S. EPA, 1998; Jun et al., 2009; Obiri-Nyarko et al., 2014). The typical building material of a PRB is zero-valent iron (Plagentz *et al.*, 2006; Jun *et al.*, 2009) in which the contaminants are degraded through a series of reduction reactions. These reduction reactions are greatly unselective and may frequently lead to solid precipitation deriving from inorganic reduction. This undesired event can seriously affect the barrier efficiency as it drastically reduces its porosity and conductivity; it can also increase the formation of preferential flow paths that lead to a reduction of the contact time of the contaminated water with the reactive material (Mackenzie *et al.*, 1999). A very promising class of PRB, which overcome this problem, is the so-called Permeable Adsorptive Barrier (PAB), in which a porous adsorbent solid is used as constituting material (Erto et al., 2011). For this specific application, activated carbon is the most widely used adsorbent (Lorbeer et al., 2002; Di Natale et al., 2008; Yang et al., 2010; Erto et al., 2011), although different classes of materials have been tested in the years, including clinoptilolite (Park et al., 2002) and fly ash

(Komnitsas et al., 2006). A PAB represents a versatile device that can be used to capture both heavy metals (Park et al., 2002; Di Natale et al., 2008) and organic compounds (Plagentz et al., 2006; Erto et al., 2011), and it is also effective when a multiple contamination is present (Erto et al., 2014). In general, the US EPA has approved adsorption on activated alumina and ion exchange as appropriate treatment methods for removing thallium from water (Peter and Viraraghavan, 2005). However, a wider selection of technologies has been investigated and reported in the literature, which also include adsorption on different types of adsorbents such as carbon nanotubes (Pu et al., 2013), hydrous manganese dioxide (Wan et al., 2014) and biomass (Peter and Viraraghavan, 2008). Adsorption is one of the most efficient and cost-effective methods for the removal of contaminants from waters (Erto et al., 2009). In particular, when contaminant concentrations are low and variable over a large area, as it is the case for groundwater, activated carbons can be considered as an optimal choice, because they are usually characterized by best performances. Consequently, the use of an activated carbon PAB for the remediation of a Tl-contaminated aquifer appears as an effective solution for both restoration and long-term protection, however specific applications for thallium removal are currently absent in the pertinent literature.

Thorough planning to ensure a correct PAB installation should include a detailed study of the geologic and hydraulic properties of the aquifer as well as a preliminary study of the adsorption performances of the adsorbent selected as PAB material. Moreover, an appropriate algorithm for the optimization of the intervention should be applied in order to make it as cost-effective as possible (Di Nardo et al., 2014; Santonastaso et al. 2017).

In this study, the remediation of a thallium-contaminated aquifer via an activated carbon PAB is proposed. The aquifer under analysis is situated in the metropolitan area of the north of Naples (Italy) in which an enormous amount of different types of waste was discharged in the past years. Following the previously indicated outline, the study started from a complete site characterization, aimed at obtaining some important PAB design parameters (e.g. piezometry and hydraulic conductivity of the aquifer). Simultaneously, a laboratory study was carried out to investigate the

adsorption properties of a commercial activated carbon for thallium removal. A simulation-based procedure implemented in COMSOL Multiphysics® was used to design the most appropriate PAB configuration, including both the conventional continuous (PAB-C) and the innovative discontinuous (PAB-D) set-ups. Moreover, a methodological approach to optimization was applied in order to define the most cost-effective configuration. The optimal dimensions of the PAB, allowing for both decontamination and long-term aquifer protection, were determined by including the dynamics of the aquifer with the contribution of the barrier itself in the same framework, from both hydraulic and chemical points of view. Finally, the optimised PAB-D was compared to an optimised continuous barrier (PAB-C), designed for the same area.

2. PAB design: model set-up

2.1. Site description

The method proposed starts with a detailed hydrogeological and hydraulic characterization (e.g. determination of soil properties, aquifer depth, etc.) of the site chosen for the case study, including the number and nature of the contaminants present and their spatial distribution.

The case study is an area of about 140 ha in Castel Volturno, a town located in north-west of Naples, Italy (Figure 1). The aquifer is northern limited by Mt. Massico and included between Tirrenean Sea and Southern Apennines, reaching the Volturno river plain in south direction. A detailed description of the area and the reference basin is reported in Corniello and Ducci (2014).

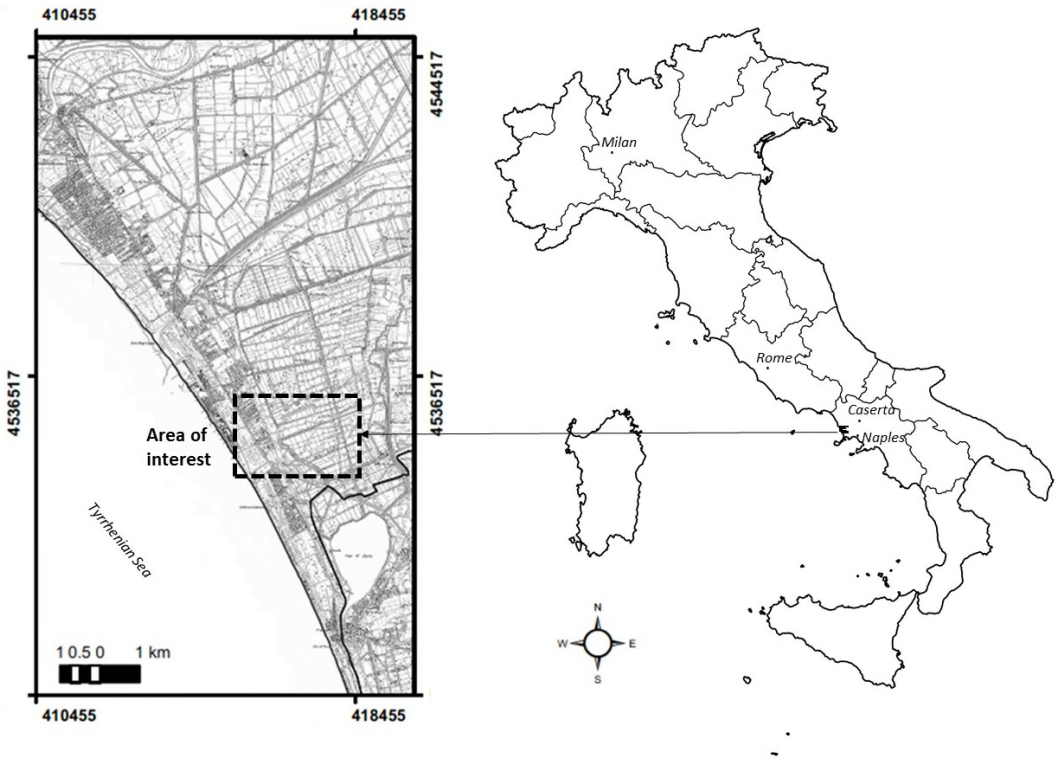

Figure 1. Position of the area of interest.

A site investigation campaign showed that a 10 m thick aquifer is present, approximately 1 m below the soil surface. The presence of natural basins and reservoirs created by anthropic activities, mostly related to agricultural practices, strongly influences the water flow and the piezometric surface trend. Groundwater pH resulted constant throughout the domain and equal to 7, as expected. In addition, numerous organic and inorganic (e.g. heavy metals like arsenic, manganese, etc.) contaminants were found in the groundwater aquifer (Ducci et al., 2017) that could be attributed to both natural and anthropogenic sources, such as landfills (mostly uncontrolled) and storage sites, animal husbandry and to a massive use of pesticides and fertilizers in the region (Cuoco et al., 2015). In particular, among heavy metals, thallium is present in high concentrations. This could be due to the inclusion of the site in the so-called "Land of Fires", a wide zone situated in the north of Napoli (D'Alisa et al., 2017), where illegal fires and sites of toxic waste incineration have been reported over the last few years.

In Figure 2, the thallium iso-concentrations, sketched based on the site investigation data, are reported, together with the map of the area and the groundwater hydraulic heights.

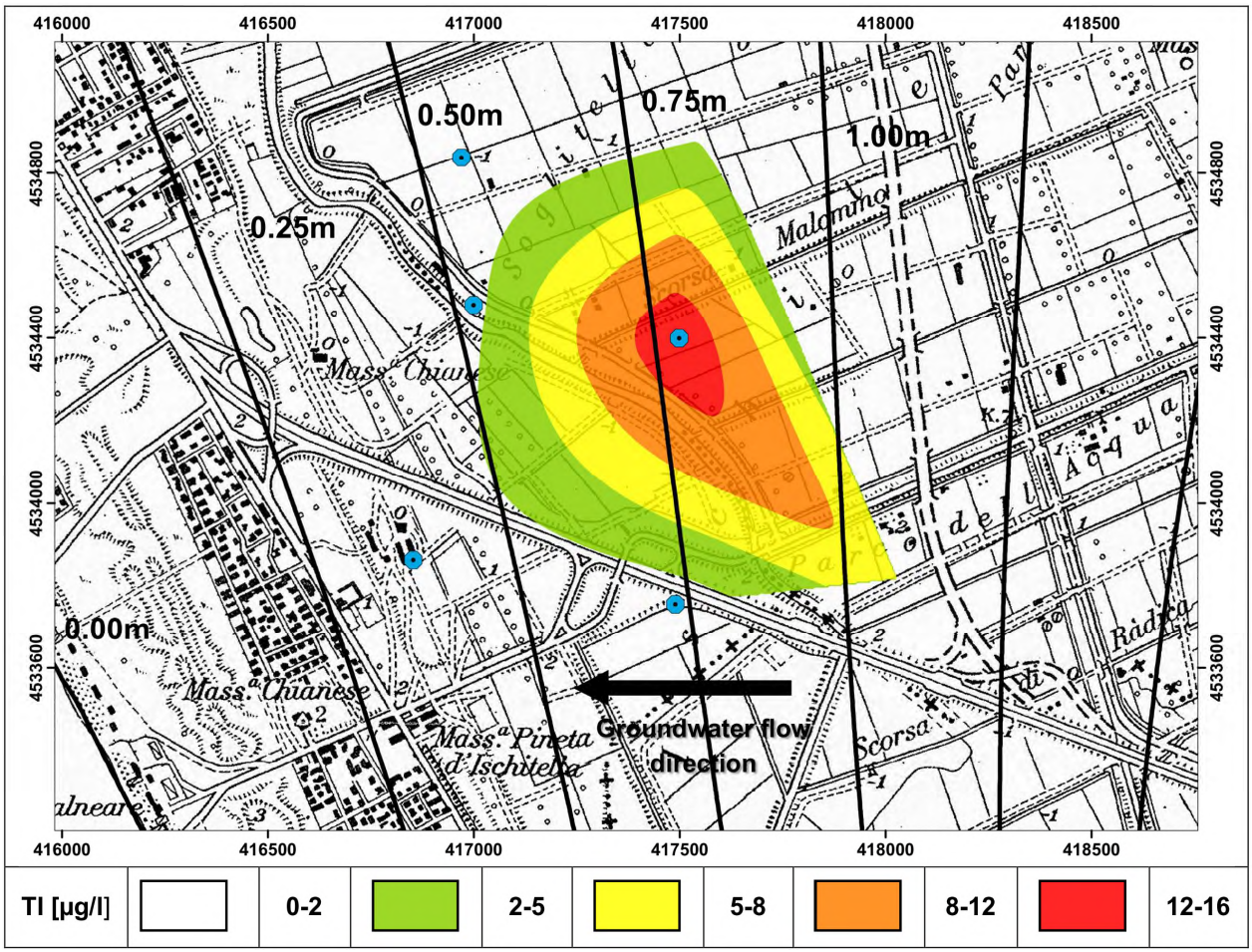

Figure 2. Thallium iso-concentrations and piezometric levels in the area of interest. The blue dots ( ) represent the wells of investigation while the black lines ( ) are the isopiezic lines.

As shown in Figure 2, in the area of interest thallium concentrations span over a wide range, with a peak that is about 7 times higher than the Italian regulatory limit (C_{lim}) - 2 µg L^{-1} - for groundwater quality. The groundwater flow lines are east-west oriented, with piezometric heights ranging between 0.25 m to 1.25 m above sea level, under a piezometric gradient (J) of 0.01m/m.

The soil composition of the site can be ascribed to alluvial, pyroclastic and marine porous sediments (i.e. silica sands), overlying the "Campanian Ignimbrite" tuffs, with a hydraulic conductivity of $2*10^{-4}$ m s^{-1} and a transmissivity of 10^{-3} m^2 s^{-1} (Corniello and Ducci, 2014). In Table 1, the hydrogeological properties of the aquifer are summarized.

Aquifer characteristics	unit	
Contaminated total area extent, A	km^2	1.39
Piezometric gradient, J	m m^{-1}	0.0005
Porosity, n_s	-	0.3
Dry soil bulk density, ρ_s	kg m^{-3}	1500
Hydraulic conductivity, K_s	m s^{-1}	0.0002
Longitudinal dispersivity, α_L	m	1
Transverse dispersivity, α_T	m	0.1
Molecular diffusion coefficient, D_d^*	m^2 s^{-1}	10^{-8}
Transmissivity, T_r	m^2 s^{-1}	10^{-3}
PAB filling material properties		
Adsorbing media		Activated Carbon
Dry bulk density, ρ_b	kg m^{-3}	520
Porosity, n_b	-	0.4
Hydraulic conductivity, K_b	m s^{-1}	0.01

Table 1. Hydrogeological properties of the aquifer and properties of the PAB filling material.

2.2. PAB configurations

The most common PAB configuration is a continuous trench (PAB-C) having length (*L*), thickness (*W*) and height (*H*) sufficient to catch the entire contaminant plume. This solution has a wide applicability, even if a limit is imposed by the extent of the excavation (Gavaskar et al., 2000; Obiri-Nyarko et al., 2014). As an alternative, when the contaminant plume is not homogenous in terms of spatial distribution, a semi-continuous barrier (PAB-S) can be used (Di Nardo et al., 2014). This configuration consists in a sequence of several sections, each with a different width, tuneable to different contaminant concentrations reaching the barrier. However, these solutions are hardly feasible since require large volume excavations; hence, several additional and innovative configurations have been proposed in the last decade (Hudak et al., 2008; Obiri-Nyarko et al., 2014). A further alternative is a discontinuous barrier (PAB-D), schematized in Figure 3. It consists

in one or more lines (n_c), orthogonal to the flow direction ($\vec{u}$) and contaminant plume, or forming a certain angle with the groundwater flow (ε), put at a certain distance (d_c), formed by a certain number (n_w) of deep passive wells, each one having a diameter (D_w), put at a distance (I), and each one filled with an adsorbent solid (Bortone et al., 2013b). Further details about the geometric properties of the barriers are reported in Di Nardo et al. (2014). This is a very attractive option as it allows a saving of filling material (Hudak, 2017).

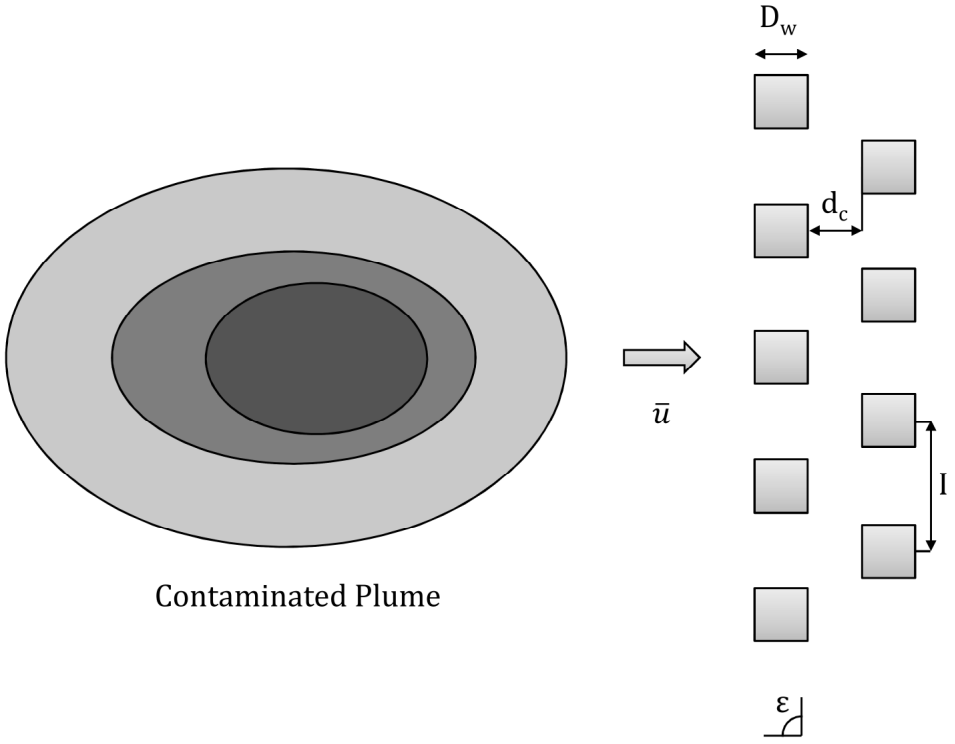

Figure 3. PAB-D Design Parameters (Bortone et al. 2013).

Similar to PAB-C and PAB-S, the PAB-D has a hydraulic conductivity higher than the surrounding soil, coercing the contaminated groundwater to flow towards the wells, where the adsorbent solid captures the contaminants.

Regardless of the configuration chosen, the performance of a PAB depends on its appropriate placement in the contaminated area. Generally, the PAB should be located as close as possible to the contaminant plume, with transversal dimensions tailored to intercept it entirely, and with an orientation orthogonal to the groundwater flow lines (Craig et al., 2006). To this aim, the real

hydraulic capture zone of a PAB, especially for PAB-D, must be accurately determined in order to ensure the capturing of the whole contaminated groundwater flow. Simultaneously, an effective design requires an accurate and comprehensive understanding of the groundwater flow regime as affected by the emplaced PAB.

An iterative procedure is applied to determine the geometrical parameters (e.g. W for a PAB-C and D_w, I, n_c, n_w for a PAB-D) allowing for a sufficient residence time within the PAB to ensure that the adsorption reactions occur. As an example, the PAB-D well diameter (D_w) is determined by the residence time required to reduce contaminant concentration below the regulatory limit. When a well diameter (D_w) is set, in order to limit the excavation burden, the determination of the optimal number of well lines (n_c) is the final target to reach for an efficient and cost-effective intervention, while the number of wells per line (n_w) is mainly determined by the extent of the contaminant plume (Bortone et al., 2013b). Although the possible solutions are potentially infinite, an algorithm is helpful to calculate the solution employing the least amount of built material (i.e. solid adsorbent) and, consequently, to result in the minimum costs (Santonastaso et al. 2016).

For each barrier configuration, it is essential to check that the contaminant concentrations downstream of the PAB (C_{out}) are lower than a fixed limit value (C_{lim}), corresponding to the established groundwater quality standard for all of the time and all over the computational domain. Eventually, as the contaminant concentration at the barrier inlet may vary during the barrier working period, the occurrence of desorption phenomena within the barrier must also be taken into consideration. In fact, if the inlet concentration decreases, it is possible that there will be contaminant release phenomena from the barrier. In this case, a higher W or n_c ensures lower outbound contaminant concentration, avoiding undesired values above the set limit (Erto et al., 2011). In this way, the PAB is dimensioned to allow for the simultaneous remediation of the aquifer and its long-term protection.

2.3. PAB modelling equations

PAB modelling includes the description of the aquifer dynamic, also accounting for the presence of the barrier itself, which exerts a double effect: alteration of the groundwater hydraulic regime and modification of the concentrations due to the capture of the contaminants by adsorption. The equation set was presented in a previous work (Erto et al., 2011) and recently adapted for the implementation in COMSOL Multiphysics® (Bortone et al., 2015). Briefly, the transport and fate of a contaminant under the influence of a PAB is described by a contaminant mass balance, which, under the hypothesis of a constant concentration profile throughout the height of the aquifer (i.e. along z-dimension), is written as:

$$\frac{\partial C}{\partial t}+\frac{\rho_b}{n_b}\frac{\partial \omega}{\partial t}-\frac{\vec{u}\nabla C}{n_b}-\nabla(D_h\nabla C)=0 \quad (1)$$

where C represents the contaminant concentration in the fluid, $\vec{u}$ the unit flux vector, D_h the hydrodynamic dispersion coefficient, ω the contaminant concentration on the solid, while ρ_b and n_b are the dry adsorbing material bulk density and porosity, respectively. The hydrodynamic dispersion coefficient is expressed as the sum of the mechanical dispersion and the molecular diffusion, hence defined by the equation:

$$D_h = D + D_d^* \quad (2)$$

in which D is the tensor of mechanical dispersion (as a function of longitudinal and transverse dispersivity coefficients, α_L and α_T, respectively) and D_d^* is the coefficient of molecular diffusion (a scalar). The molecular diffusion effect is usually negligible as compared to the mechanical dispersion effect, and becomes important only when groundwater velocity is very low (Erto et al., 2011).

The unit flux vector $\vec{u}$ can be determined by the application of the Darcy equation, applied to water flow in either the aquifer or the barrier, as:

$$\vec{u} = -K_S \cdot \vec{\nabla} h \text{ or } \vec{u} = -K_b \cdot \vec{\nabla} h \quad (3)$$

in which K_s is the soil hydraulic conductivity, K_b is the barrier hydraulic conductivity and h is the hydraulic load. This latter is calculated via the Laplace Eq. (4), with appropriate boundary conditions:

$$-\frac{\partial^2 h}{\partial x^2}-\frac{\partial^2 h}{\partial y^2}-\frac{\partial^2 h}{\partial z^2}=0 \tag{4}$$

The second term on the left of Eq.(1) describes the adsorption phenomena occurring on the solid surface and can be written as:

$$\frac{\rho_b}{n_b}\frac{\partial \omega}{\partial t}=k_c a\left[C-C^*(\omega)\right] \tag{5}$$

where a is the specific surface area of the sorbent, calculated as the surface area/volume ratio of the adsorbent particle hypothesized as spherical (i.e. a= $6/d_p$, in which dp is particle diameter). k_c is the contaminant mass transport coefficient that, due to the general low Reynolds number of groundwater flow and considering small adsorbent particle size, can be approximated to the value occurring in the film fluid surrounding the particle (Bortone et al., 2013b). Finally, $C^*(\omega)$ represents the equilibrium concentration in correspondence of the solid adsorption capacity (ω) obtained from the adsorption isotherm of the contaminant under analysis on the chosen adsorbent. It defines the mass transfer driving force (i.e. the concentration gradient) in the transport equation.

As to initial conditions, the contaminant liquid concentration in the whole area is previously determined throughout the entire flow domain and the initial contaminant concentration onto the sorbent material is assumed to be equal to zero; the overall boundary conditions can be expressed as follows:

$$\begin{cases} x=0 & C=0 & \forall y,\forall z,\forall t \\ y=0 & C=0 & \forall x,\forall z,\forall t \\ y=Y & C=0 & \forall x,\forall z,\forall t \\ x=X & \dfrac{\partial C}{\partial t}+\dfrac{\vec{u}\nabla C}{n_s}-\nabla(D_h\nabla C)=0 & \forall y,\forall z,\forall t \end{cases} \tag{6}$$

The reference frame is assumed to coincide with the boundary of the domain, and then X is defined as the distance between the barrier and the axis origin, while Y is the size of the domain in y direction.

The entire set of equations was resolved with COMSOL Multi-physics® via adopting different modelling scales for transport (Eq.1) and adsorption (Eq.5), in order to simulate the dynamics of the system over a period of many years.

3. Thallium adsorption: lab-scale tests

For a proper design of a cost-effective adsorption system, such as that of a PAB, it is mandatory to accurately assess the adsorption capacity of the PAB reactive media (i.e. the solid adsorbent) under experimental conditions as close as possible to those of the aquifer. Moreover, as stated in the previous section, the equation set used to design the PAB for groundwater treatment requires the definition of appropriate theoretical models (i.e. adsorption isotherms) for thallium adsorption. To this aim, dedicated lab-scale adsorption tests were performed, according to the methodology reported in the following.

3.1. Materials

The adsorbing material used in the lab-experiments was the Aquacarb 207EA™. This is a commercially available non-impregnated granular activated carbon (GAC), produced by Sutcliffe Carbon starting from a bituminous coal (Table 1). This material has a narrow particle size distribution with an average diameter of 1.2 mm, a BET surface area of 950 $m^2\ g^{-1}$ and a micropore volume of 0.249 $cm^3\ g^{-1}$ (Erto et al., 2010). Dry bulk density (ρ_b) is about 500 $kg\ m^{-3}$, porosity (n_b) is 0.4 $m^3\ m^{-3}$ and hydraulic conductivity is about 0.001 $m\ s^{-1}$. Sorbent particles with average diameter between 1.2-1.4 mm were sieved. Before each experimental run, the sorbent was carefully rinsed with distilled water and oven dried for 48 h at 120°C.

3.2. Experimental

Isotherm experiments were conducted in batch mode in a P.I.D. controlled thermostatic oven at temperature levels between 10 and 50°C and constant pH (neutral). Stock solutions of thallium (I) were prepared by dissolving thallium chloride (TlCl, 99% Sigma Aldrich) in distilled water. Each sample consists of a 100 mL of thallium solution at initial concentration in the range 0.5-10 mg L^{-1}, in contact with a 0.5 g of sorbent. Preliminary kinetic tests indicated a time range of 72 h to reach thermodynamic equilibrium. At equilibrium, both thallium concentration in solution and thallium adsorbed on the carbon surface were measured; to such a purpose, the carbon was leached with 100 ml of nitric acid (1 M) for a complete thallium extraction. The experimental run accuracy was checked by allowing for a maximum error of 5% in the thallium mass balance. Thallium concentrations were measured by means of air/acetylene flame atomic absorption spectrophotometry (AAS-F) via using a Varian SpectrAA-220 spectrophotometer.

4. Results and discussion

4.1. Thallium (I) adsorption isotherms

Because the groundwater temperature can vary depending on the aquifer properties, the effect of temperature on thallium adsorption onto activated carbon was investigated at different temperatures. In Figure 4, the thallium adsorption isotherms on Aquacarb 207EA® GAC at 10, 20 and 50 °C, and a constant value of pH=7 are reported.

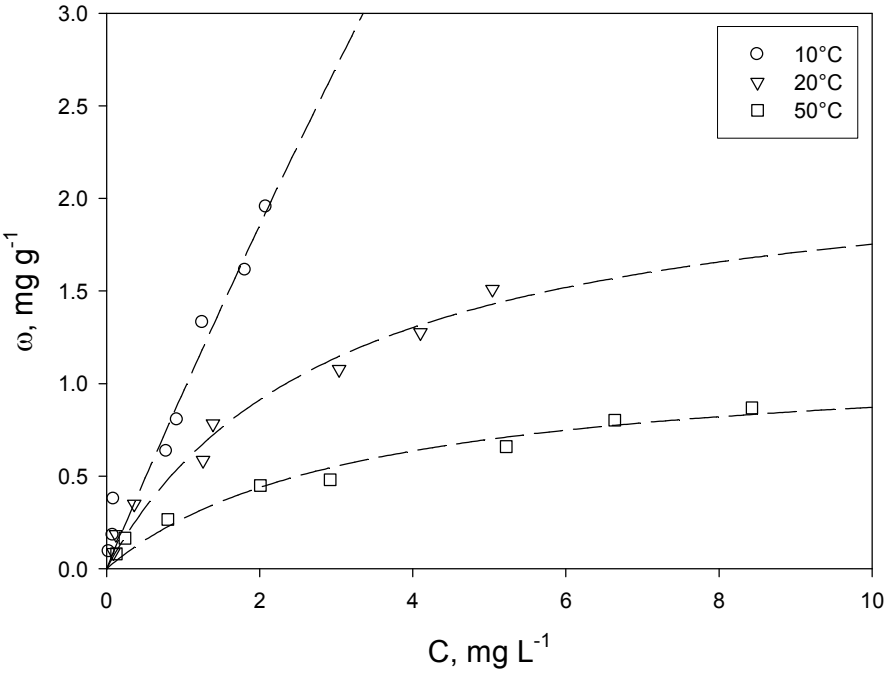

Figure 4. Thallium (I) adsorption isotherms onto Aquacarb 207EA™ GAC as a function of temperature (Equilibrium pH=7). Comparison Langmuir model results (lines).

As expected, thallium (I) adsorption shows the characteristic exothermic trend and significant decrease of adsorption capacity occurs by increasing the temperature.

A data regression analysis on experimental data set was carried out using the Langmuir model while the best fitting model parameters were determined using the least residual sum-of-squares criterion. The Langmuir adsorption equation is written as:

$$\omega = \omega_{\max} \frac{KC}{1 + KC} \tag{7}$$

where ω_{max} and K are maximum adsorption capacity and Langmuir constant, respectively. The effectiveness of the model fitting was assessed through the standard error (*Std error*) and the coefficient of determination (R^2). The values of regression parameters of the Langmuir model, with their error of determination, are reported in Table 2:

T [C]	*Langmuir parameters*	*Mean*	*Std error*	R^2
10	ω_{max} [mg g^{-1}]	$3.46\ 10^{1}$	$1.46\ 10^{2}$	0.956
	K [L mg^{-1}]	$2.83\ 10^{-2}$	$1.25\ 10^{-1}$	
20	ω_{max} [mg g^{-1}]	2.27	$3.27\ 10^{-1}$	0.976
	K [L mg^{-1}]	$3.34\ 10^{-1}$	$9.92\ 10^{-2}$	
50	ω_{max} [mg g^{-1}]	1.16	$1.37\ 10^{-1}$	0.967
	K [L mg^{-1}]	$3.04\ 10^{-1}$	$8.84\ 10^{-2}$	

Table 2. Langmuir model parameters from regression analysis of thallium adsorption on Aquacarb 207EA

These parameters are an essential part of model application for the design of PABs via using software simulations.

4.2. PAB design results

Once the hydraulic and geochemical characteristics of the aquifer are known and the adsorption properties of the adsorbent are determined, it is possible to plan and optimize the remediation intervention via PAB application. In fact, these parameters significantly affect the determination of the optimal PAB geometrical parameters, as extensively demonstrated in Bortone et al. (2015).

Moreover, it is not possible to define *a priori* the best PAB configuration for the specific case study among those listed above (cf. Paragraph 2.2) as, for each of them, many different solutions are technically effective (i.e. allowing for the effective capture of the contaminant plume so as to ensure a concentration lower than the regulation limits downstream of the PAB itself). For this reason, a systematic comparative analysis should include other important parameters such as technical feasibility, commercial availability and, last but not least, economic impact. It is worth

observing that, based on the initial contaminant plume distribution in the area, a partial pre-selection opting for either PAB-C or PAB-D configurations is possible, as the PAB-S can be dismissed for its impractical feasibility due to the complexity of the excavation step (Di Nardo et al., 2014). Then, the complete evaluation of each configuration and of the corresponding optimal parameters can be done only through numerical simulations using the set of Eqs (1)-(5) and the boundary conditions expressed by Eq. (6). In addition, the design procedure implicitly involves the definition of the optimized solution for both configurations (i.e. PAB-C or PAB-D), in line with the criteria illustrated in the paragraph 2.2.

A meaningful comparison should take into account the minimum PAB volume needed, as a basic step for an economic optimization, because the cost of the adsorbing material has a major influence on the overall costs of PABs' installation (Bortone et al., 2014). However, when different configurations are considered, the excavation costs can be a discriminating factor, in particular when different geometric solutions are considered (e.g. different well diameters), as reported by Santonastaso et al. (2017).

The first simulations aimed at identifying the optimal dimensions of a PAB-C located at a distance equal to 10 m from the contaminant plume, with a north direction orientation (ε). The PAB-C length (L=1077 m) was defined by following the contaminant initial plume distribution (Figure 2) and its flow migration over the time, while the optimized thickness (W=2.85 m) was obtained via an iterative procedure (Di Nardo et al., 2014) where the PAB-C thickness, W, was increased of a ΔW step equal to 0.1 m each simulation. Subsequently, new simulations were carried out in order to design a PAB-D and an optimization procedure was substantial to minimize the intervention and the overall costs. All PAB simulations were carried out assuming a groundwater temperature equal to 10°C.

As described in paragraph 2.2, a PAB-D is characterized by a higher number of geometrical parameters and variables (i.e. D_w, I, n_c, n_w) that have to be optimized, compared to a PAB-C (i.e. W and L). As expected, these parameters are strictly interconnected (for example, a higher well

diameter can determine a lower number of wells, thus potentially a lower PAB-D volume to complete the intervention). Hence, their optimization requires a series of further consecutive dedicated simulations and cannot be predicted via theoretical arguments.

The first optimization step aimed at determining the optimal well diameter (D_w). This is the most important parameter, exerting a significant influence on both the excavation operating parameters and extent of the intervention. The choice was restricted to those diameters that are technically feasible (i.e. compatible with the typical dimensions of the existing excavation machines). In Table 3, the possible diameters identified through a preliminary technical survey are reported, together with their cost of excavation (C_{well}), based on the local market indications. The unit costs of a typical adsorbent medium (e.g. activated carbon) (C_{Ad}) and PAB-D monitoring costs (C_M) were also indicated, for the subsequent economical evaluations.

D_w [m]	C_{well} unit cost [€ m^{-1}]	C_{Ad} unit cost [€ m$^{-3}_{Ad}$]	C_M [€]
0.8	69	780	250,000
1.0	87		
1.5	122		
2.0	158		

Table 3. PAB-D costs: unit cost of well excavation (C_{well}), unit cost of adsorbent (C_{Ad}) and PAB monitoring costs (C_M)

A following step of the PAB-D optimization procedure aimed at investigating the effect of the well-to-well distance (I). In particular, in order to reduce the number of simulations, for each possible well diameter, a D_w-dependent line-to-line distance (i.e. $d_c = D_w$) was assumed and two different well-to-well distances (i.e. $I = 2D_w$ and $I = 4D_w$) were tested, according to the scheme reported in Table 4:

Configuration		D_w [m]	I [m]	d_c [m]
$I=2D_w$	1	0.8	1.6	0.8
	2	1.0	2.0	1.0
	3	1.5	3.0	1.5

	4	2.0	4.0	2.0
$I=4D_w$	5	0.8	3.2	0.8
	6	1.0	4.0	1.0
	7	1.5	6.0	1.5
	8	2.0	8.0	2.0

Table 4. PAB-D configurations tested for the diameter D_w optimization

In addition, further iterative simulations aimed at determining the number of PAB-D lines (n_c), for each PAB-D configuration indicated in Table 4. In particular, consecutive well lines were added in the groundwater flow direction until the thallium outlet concentrations became lower than the corresponding regulatory limit in the entire domain (Bortone et al., 2013b). In this way, it was possible to determine the minimum total PAB-D number of wells (n_w), and consequently the minimum PAB-D volume, also ensuring both the compliance with the groundwater protection standard downstream of the barrier and the long-term aquifer protection.

In Table 5, the simulation results for the eight PAB-D configurations are illustrated with the main geometrical parameters and costs obtained. For all configurations, a PAB-D height, H, equal to 10 m was assumed.

Configuration	D_w **[m]**	n_c	n_w	V_{Ad} **[m^3]**	C_{well} **[€]**	C_{Ad} **[€]**	C_T **[€]**
1	0.8	8	3,454	22,106	2,621,586	17,242,368	19,863,954
2	1	6	2,258	22,580	2,160,906	17,612,400	19,773,306
3	1.5	4	1062	23,895	1,425,204	18,638,100	20,063,304
4	2	3	630	25,200	1,094,940	19,656,000	20,750,940
5	0.8	16	3,241	20,742	2,459,919	16,179,072	18,638,991
6	1	12	1,990	19,900	1,904,430	15,522,000	17,426,430
7	1.5	8	922	20,745	1,237,324	16,181,100	17,418,424
8	2	6	578	23,120	1,004,564	18,033,600	19,038,164

Table 5. Results of the PAB-D optimisation

As shown in Tables 4 and 5, for each well-to-well distance (I) tested, an increase in D_w entailed a monotonic decrease of the number of well lines (n_c), due to the correlated rise of the overall

adsorbing material width along the groundwater flow direction. At the same time, a decrease of the number of total wells per configuration (n_w) was observed; this was due to the reduction of the thallium outlet concentration per well line as a consequence of the bigger wells' adsorptive action and of the different consequent thallium plume evolution over the time. In addition, by increasing the well-to-well distance (I), a further reduction of the total number of wells for a same D_w was observed, even if a decreasing linear trend was not followed.

In general, for each well diameter, by increasing I, a significant increase of the number of well lines (n_c) can be observed (variable with the well diameter). However, the total number of wells was always lower, because of the optimized solution. In other words, a higher number of wells in the groundwater flow direction (i.e. increase of n_c) showed to be more effective than a higher number of wells in each line (i.e. when D_w decreases).

The total volume of adsorbing material follows different trends as a function of I. For $I= 2D_w$, the reduction of the number of wells does not compensate for the increase in the well diameter, hence the total volume of adsorbing material (V_{Ad}), monotonically rises with the well diameter itself. Differently, for $I= 4D_w$, the total volume of adsorbing material has a minimum value (corresponding to solution #6, with D_w = 1 m), which was not expected. This is a very interesting result suggesting a test of the behaviour of the system in correspondence to a further increase in I; however, it is worth observing that these tests would imply a significant increase in the number of well lines (cf. Table 5) and, consequently, in the extension of the intervention in the groundwater direction. For this reason, even if theoretically interesting, these tests were not carried out. Hence, for the PAB-D configurations investigated, the minimum of the total volume of adsorbing material was found in the solution #6, with D_w = 1 m, which was considered as the optimum in terms of total volume of adsorbing material.

In a second stage of the analysis of simulation results, a costs analysis was carried out. As reported in Table 5, C_T is the total cost of the intervention, defined as the sum of the cost of excavation and the cost of adsorbent ($C_T= C_{well} + C_{Ad}$). These costs were evaluated based on the unit

values reported in Table 3. For C_{well}, a total excavation height of 11 m was considered (being each well 10 m high and built 1 m below the soil surface). It is also specified that the monitoring costs should be added once the final costs are determined. They were not included at this stage, as they are considered as constant for each configuration tested and do not allow for discriminating the different solutions.

As it is possible to observe in Table 5, at a constant D_W, an increase in the well-to-well distance (I) determines a decrease of both adsorbing material and total intervention costs. However, for bigger I, the excavation costs (C_{well}) have a major influence and indicate solution #7 as the optimum. In fact, when D_w increases from 1 m to 1.5 m, the reduction of C_{well}, due to the related minor number of n_w in the PAB-D array, largely counterbalances the C_{Ad} growth, which is directly dependent upon the well diameter. For the same reason, for $I= 4D_w$, the total costs of intervention are lowest; in this case, the reduction in n_w determines both a C_{well} (as previously observed) and C_{Ad} decrease. In conclusion, for the investigated case-study, the lowest overall cost can be obtained via achieving a good compromise between the total number of wells and their dimension, the former parameter having the greatest influence.

It is worth observing that these results are valid for the specific case-study and cannot be generally extended, except for the optimization methodology, as they are strictly dependant on the values of some of the design parameters (i.e. n_w, n_c, etc.). In turn, these parameters depend on the hydrogeological characteristics of the aquifer, on the shape and extension of the contaminant plume and on the concentration values considered, as extensively demonstrated.

For the optimised PAB-D configuration, further results of the numerical simulations were reported. In fact, in order to prove the effectiveness of the barrier, the evolution over run time of contaminant spots in the form of snapshots taken every 20 years can be depicted in Figure 5.

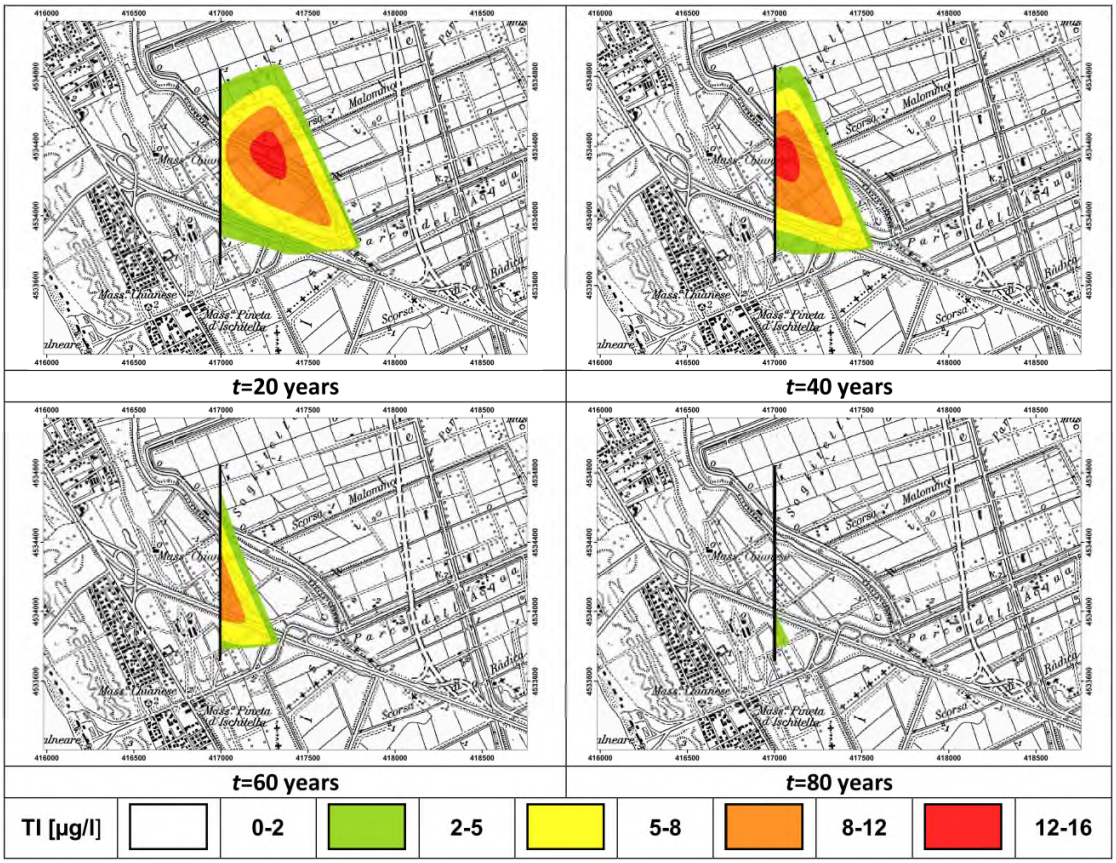

Figure 5. Thallium iso-concentration into the aquifer as a function of the working time

Figure 5 shows that the contaminant is efficiently captured as the contamination approaches the barrier; indeed, at any run time the thallium concentration downstream of the barrier is always lower than the regulatory limit (2 µg L^{-1}). The total restoration of the aquifer can be achieved in approximately 80 years; however, it is important to note that this long restoration period is due only to the hydraulic properties of the aquifer and not to inefficacy of the remediation method. Furthermore, dealing with a PAB filled with activated carbon, the possible desorption of the previously adsorbed thallium may occur (Erto et al., 2011). In particular, this becomes plausible when the thallium concentration approaching the barrier decreases over the time (or becomes approximately zero when the aquifer is restored), so that the corresponding concentration onto the barrier could be higher than the equilibrium value, retrievable from the adsorption isotherm. However, the simulation algorithm used considers this event. In Figure 6, the thallium concentrations over the run time, respectively at the PAB-D inlet (C_{in}) and outlet (C_{out}) along the

groundwater flow direction, where the highest thallium concentrations flowed through the barrier were detected, are illustrated (breakthrough curves). The thallium concentration limit (C_{lim}) fixed at 2μg L^{-1} is also reported for a direct comparison.

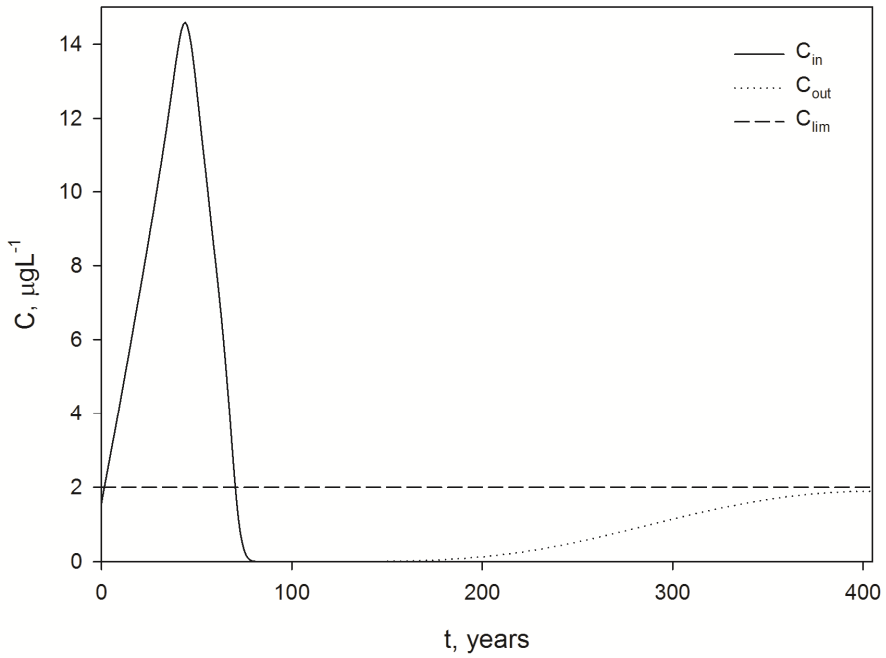

Figure 6. Breakthrough curve for thallium concentration at the inlet (C_{in}) and at the outlet (C_{out}) of the barrier. Italian regulation limit (C_{lim}) for thallium concentration in groundwater is also reported

Results in Figure 6 show that the inbound thallium concentration changes during the run time, reaching a maximum after about 40 years and maintaining a concentration higher than C_{lim} for approximately 80 years, after which the plume disappears. In the same period, it is confirmed that the aquifer is completely restored as the outbound thallium concentration (C_{out}) is always far lower than the concentration limit (C_{lim}). Moreover, the Tl concentration values stay below the regulation limit for much longer time, showing that the PAB-D is designed to tackle a possible occurrence of desorption phenomena from the saturated barrier toward the aquifer, after that the whole contamination was captured.

Finally, the optimized PAB-D configuration was compared with a PAB-C for the remediation of the same case study. In particular, the evaluation was made over ΔV_{Ad}, i.e. the volume percentage reduction of the adsorbent material needed for to build the PAB-D in contrast with the PAB-C, and ΔC_T, i.e. the corresponding difference in the overall intervention costs. In Table 6, the design and related economic values for both the optimised PAB-C and PAB-D obtained for the case study, are shown.

	Height [m]	**Width [m]**	**Length [m]**	**V_{ad} [m^3]**	**ΔV_{ad} [%]**	**C_T [€]**	**ΔC_T [%]**
Optimised PAB-C	10	2.85	1,077	30,695	-	27,025,461	
Optimised PAB-D	10	1.5	-	20,745	32	17,418,424	36

Table 6. Comparison between optimised PAB-C and PAB-D results

Using a PAB-D configuration allows for a significant saving (about 36%) of adsorbing material and, consequently, a considerable reduction of the total costs for site remediation as compared to the PAB-C.

5. Conclusions

This work dealt with the design of permeable adsorptive barriers (PABs) for the restoration of an aquifer situated in the area north-west of Naples (Italy), in which a thallium (I) contamination was detected. The aquifer is situated in the so-called "Land of Fires" in which a wide and multiple groundwater contamination is present. The study was carried out under the simplified hypothesis of single contamination by thallium and aimed at the definition of an optimized PAB configuration, in terms of groundwater restoration and minimum costs. A preliminary dedicated laboratory study was carried out to assess the adsorption capacity of an activated carbon to use as PAB adsorbing filling material. The experimental tests allowed for a determination of the adsorption capacity as a function of water temperature, also providing the modelling data to describe the adsorption phenomena occurring into the barrier. The design of the barrier was performed via simulations carried out in

COMSOL Multiphysics®, for which a preliminary assessment of the hydraulic and geological properties of the site was necessary. Different barrier configurations were tested, either as continuous trench or as discontinuous array of wells. An optimization procedure was applied to define the well diameter (D_w) and the well-to-well distance (I). Results show that at a constant well diameter, an increase in the distance between wells determines a significant increase in the number of well lines but also a reduction in the total number of wells. Furthermore, by increasing the well diameter, a significant reduction in the total number of wells was obtained, however, without reducing the total volume of adsorbing material. The optimized PAB-D configuration where the total volume of adsorbing material is minimum, occurred for the higher well-to-well distance tested ($I=4D_W$) and D_w = 1 m.

Although, by estimating the total costs of intervention as a sum of well excavation (C_{well}) and absorbing material acquisition costs (C_{Ad}), it is ascertained that D_w = 1.5 m is the most cost-effective solution. Hence, it was concluded that, for the investigated case-study, the reduction in the total number of wells and, consequently, in C_{well} play a major role.

For this solution, the evolution over run time of the contaminant spots proved that the designed PAB-D is able to perform a complete aquifer restoration in approximately 80 years. Moreover, the barrier was also designed to tackle the possible desorbing phenomena occurring after the contaminant has been completely captured; indeed, for a longer operating time, the thallium concentration downstream of the barrier always resulted lower than the corresponding regulation limit.

Finally, the simulation results clearly showed that the discontinuous barrier (PAB-D) allows for a significant saving both in terms of volume of adsorbing materials and overall costs with respect to the continuous barrier (PAB-C).

References

1. Bortone, I., Chianese, S., Di Nardo, A., Di Natale, M., Erto, A., Musmarra, D., 2013a. A comparison between pump & treat technique and permeable reactive barriers for the remediation of groundwater contaminated by chlorinated organic compounds. Chem. Eng. Trans. 32, 31-36.
2. Bortone, I., Di Nardo, A., Di Natale, M., Erto, A., Musmarra, D., Santonastaso, G. F., 2013b. Remediation of an aquifer polluted with dissolved tetrachloroethylene by an array of wells filled with activated carbon. J. Hazard. Mater. 260, 914-920.
3. Bortone, I., Erto, A., Di Nardo, A., Di Natale, M., Santonastaso, G., Musmarra, D., 2014. Design of permeable adsorbing barriers for groundwater protection: Optimization of the intervention. Chem. Eng. Trans. 36, 547-552.
4. Bortone, I., Erto, A., Santonastaso, G., Di Nardo, A., Di Natale, M., Musmarra, D., 2015. Design of Permeable Adsorptive Barriers (PAB) for groundwater remediation by COMSOL Multi-physics simulations. Desalin. Water Treat. 55(12), 3231-3240.
5. Corniello, A., Ducci, D., 2014. Hydrogeochemical characterization of the main aquifer of the “litorale domizio-agro aversano NIPS”(Campania—southern Italy). J. Geochem. Explor., 137, 1–10.
6. Craig, J.R., Rabideau, A.J., Suribhatla, R., 2006. Analytical expressions for the hydraulic design of continuous permeable reactive barriers. Adv. Water Resour. 29 (1), 99–111.
7. Cuoco, E., Darrah, T.H., Buono, G., Verrengia, G., De Francesco, S., Eymold, W.K., Tedesco, D., 2015. Inorganic contaminants from diffuse pollution in shallow groundwater of the Campanian Plain (Southern Italy). Implications for geochemical survey. Environ. Monit. Assess. 187(2): 46.
8. D'Alisa, G., Germani, A.R., Falcone, P.M., Morone, P. 2017. Political ecology of health in the Land of Fires: a hotspot of environmental crimes in the south of Italy. J.Politic. Ecol. (24), 59-86.

9. Di Nardo, A., Bortone, I., Di Natale, M., Erto, A., Musmarra, D., 2014. A heuristic procedure to optimize the design of a permeable reactive barrier for groundwater remediation. Adsorpt. Sci. Technol. 32(2-3), 125-140.

10. Ducci, D., Albanese,S., Boccia, L., Celentano,E., Cervelli, E., Corniello, A., Crispo, A., De Vivo, B., Iodice, P., Langella, C., Lima, A., Manno, M., Palladino, M., Pindozzi, S., Rigillo, M., Romano, N., Sellerino,M., Senatore,A., Speranza, G., Fiorentino, N., Fagnano, M., 2017. An Integrated Approach for the Environmental Characterization of a Wide Potentially Contaminated Area in Southern Italy. J. Environ. Res Public Health, 14(7), 693-716.

11. Di Natale, F., Di Natale, M., Greco, R., Lancia, A., Laudante, C., Musmarra, D., 2008. Groundwater protection from cadmium contamination by Permeable Adsorbing Barriers. J. Hazard Mater. 160(2-3), 428-434.

12. Erto, A., Andreozzi, R., Di Natale, F., Lancia, A., Musmarra, D., 2009. Experimental and isotherm-models analysis on TCE and PCE adsorption onto activated carbon. Chemical Engineering Transactions, 17, 293-298.

13. Erto, A., Andreozzi, R., Di Natale, F., Lancia, A., Musmarra, D., 2010. Experimental and statistical analysis of trichloroethylene adsorption onto activated carbon. Chem. Eng. J. 156 (2), 353-359.

14. Erto, A., Lancia, A., Bortone, I., Di Nardo, A., Di Natale, M., Musmarra, D., 2011. A procedure to design a Permeable Adsorptive Barrier (PAB) for contaminated groundwater remediation. J. Environ. Manage. 92, 23-30.

15. Erto, A., Bortone, I., Di Nardo, A., Di Natale, M., Musmarra, D., 2014. Permeable Adsorptive Barrier (PAB) for the remediation of groundwater simultaneously contaminated by some chlorinated organic compounds. J. Environ. Manage. 140, 111-119.

16. Gavaskar, A., Gupta, N., Sass, B., Janosy, R., Hicks, J., 2000. Design Guidance for Application of Permeable Reactive Barriers for Groundwater Remediation. Alison Lightner Air Force Research Laboratory. Columbus, OH.

17. Hudak, P.F., 2008. Configuring passive wells with reactive media for treating contaminated groundwater. Environ. Prog. 27(2), 257–262.

18. Hudak, P.F., 2017. Large-diameter, non-pumped wells filled with reactive media for groundwater remediation. Environ Earth Sci.76, 667.

19. Jun, D., Yongsheng, Z., Weihong, Z., Mei, H., 2009. Laboratory study on sequenced permeable reactive barrier remediation for landfill leachate-contaminated groundwater. J. Hazard. Mater. 161(1), 224–230.

20. Komnitsas, K., Bartzas, G., Paspaliaris, I., 2006. Modeling of reaction front progress in fly ash permeable reactive barriers. Environ. For. 7, 219–231.

21. López Antón, M. A., Alan Spears, D., Díaz Somoano, M., Martínez Tarazona, M. R., 2013. Thallium in coal: Analysis and environmental implications. Fuel 105, 13–18.

22. Lorbeer, H., Starke, S., Gozan, M., Tiehm, A., Werner, P., 2002. Bioremediation of Chlorobenzene-contaminated groundwater on granular activated carbon barriers. Water, Air, Soil Pollut. Focus 2, 183-193.

23. Mackenzie, P.D., Horney, D.P., Sivavec, T.M., 1999. Mineral precipitation and porosity losses in granular iron columns. J Hazard Mater 68, 1–17.

24. Nriagu, J.O., 1998. History, production, and uses of thallium. In Nriagu J.O. (Ed.), Thallium in the environment. Advances in Environmental Science and Technology, 29 Wiley-Interscience, New York.

25. Obiri-Nyarko, F., Grajales-Mesa, S. J., Malina, G., 2014. An overview of permeable reactive barriers for in situ sustainable groundwater remediation. Chemosphere 111, 243-259.

26. Park, J.B., Lee, S.H., Lee, J.W., Lee, C.Y., 2002. Lab scale experiments for permeable reactive barriers against contaminated groundwater with ammonium and heavy metals using clinoptilolite. J. Hazard. Mater. B95, 65–79.

27. Peter, A.L. J., Viraraghavan, T., 2005. Thallium: a review of public health and environmental concerns. Environ Int, 31, 493–501.

28. Peter, A.L.J., Viraraghavan, T., 2008. Removal of thallium from aqueous solutions by modified Aspergillus niger biomass. Bioresour. Technol. 99(3), 618-625.

29. Plagentz, V., Ebert, M., Dahmke, A., 2006. Remediation of groundwater containing chlorinated and brominated hydrocarbons, benzene and chromate by sequential treatment using ZVI and GAC. Environ. Geol. 49(5), 684-695.

30. Pu, Y., Yang, X., Zheng, H., Wang, D., Sub, Y., He, J., 2013. Adsorption and desorption of thallium (I) on multiwalled carbon nanotubes. Chem. Eng. J. 219, 403-410.

31. Santonastaso, G.F., Bortone, I., Chianese, S., Erto, A., Di Nardo, A., Di Natale, M., Musmarra, D., 2016. Application of a discontinuous permeable adsorptive barrier for aquifer remediation. A comparison with a continuous adsorptive barrier. Desalin. Water Treat., 57(48-49), 23372-23381.

32. Santonastaso, G.F, Bortone, I., Chianese, S, Di Nardo, A., Di Natale, M., Erto, A., Karatza, D., Musmarra, D., 2017. Discontinuous Permeable Adsorptive Barrier design and cost analysis: a methodological approach to optimisation, Environ. Sci. Pollut. Res., In press DOI: 10.1007/s11356-017-0220-y

33. U.S. EPA (U.S. Environmental Protection Agency), 2017. Ground Water and Drinking Water-National Primary Drinking Water Regulations (last updated July 11, 2017). Available online https://www.epa.gov/ground-water-and-drinking-water/national-primary-drinking-water-regulations

34. U.S. EPA (U.S. Environmental Protection Agency), 1998. Permeable reactive barrier technologies for contaminant remediation. EPA/600/R-98/125.

35. Viraraghavan, T., Srinivasan, A., 2011. Thallium: environmental pollution and health effects. Encyclopedia of Environ Health. 325–333.

36. Wan, S., Ma, M., Lu, L., Qian, L., Xu, S., Xue, Y., Ma, Z., 2014. Selective capture of thallium (I) ion from aqueous solutions by amorphous hydrous manganese dioxide. Chem. Eng. J. 239, 200–206.

37. Yang, J., Caob, L., Guob, R., Jiab, J., 2010. Permeable reactive barrier of surface hydrophobic granular activated carbon coupled with elemental iron for the removal of 2,4-dichlorophenol in water. J. Hazard. Mater. 184(1–3), 782–787.

LIST OF SYMBOLS

a	Adsorbing material external surface area, $m^2\ m^{-3}$
A	Polluted area total extent, km^2
C	Liquid concentration, $\mu g\ L^{-1}$
C^*	Equilibrium liquid concentration, $\mu g\ L^{-1}$
C_{Ad}	Cost of adsorbing material, €
C_{in}	Barrier inflow pollutant concentration, $\mu g\ L^{-1}$
C_{lim}	Pollutant regulatory limit value, $\mu g\ L^{-1}$
C_M	Monitoring costs, €
C_{out}	Barrier outflow pollutant concentration, $\mu g\ L^{-1}$
C_T	Total cost of the intervention, €
C_{well}	Cost of well excavation, €
D	Tensor of mechanical dispersion
d_c	Distance between well lines, m
D_d^*	Molecular diffusion coefficient, $m^2\ s^{-1}$
D_h	Hydrodynamic dispersion coefficient, $m^2\ s^{-1}$
D_w	Well diameter, m
E	Distance between barrier and pollutant plume, m
H	Barrier height, m

h	Hydraulic load, m
I	Distance between wells, m
J	Piezometric gradient, m m^{-1}
K	Langmuir constant, l mol^{-1}
K_b	Barrier hydraulic conductivity, m s^{-1}
k_c	Adsorption overall mass transfer coefficient, m s^{-1}
K_s	Soil hydraulic conductivity, m s^{-1}
L	Barrier length, m
m	Barrier orientation, °
n_b	Barrier porosity
n_c	Number of well lines, -
n_s	Soil porosity
n_w	Number of wells per line, -
PAB-C	Continuous Permeable Adsorptive Barrier
PAB-D	Discontinuous Permeable Adsorptive Barrier
PAB-S	Semi-continuous Permeable Adsorptive Barrier
T	Absolute temperature, K
t	Time, yr
T_R	Transmissivity, m^2 s^{-1}
u	Groundwater flow velocity, m s^{-1}
V_{Ad}	Barrier adsorbing volume, m^3
W	Barrier thickness, m
X	Distance between barrier and western boundary of the domain, m
Y	Extension domain in y direction
α_L	Longitudinal dispersivity, m

α_T	Transversal dispersivity, m
ΔW	Barrier thickness step, m
ε	Groundwater flow direction, °
ρ_b	Activated carbon bulk density, kg m^{-3}
ρ_s	Dry soil bulk density, kg m^{-3}
ω	Activated carbon adsorption capacity, mg g^{-1}
ω_{max}	Maximum carbon adsorption capacity, mg g^{-1}

Experimental and simulation study of the restoration of a thallium (I)-contaminated aquifer by Permeable Adsorptive Barriers (PABs)

Santonastaso, G. F.

2018-02-20

Santonastaso GF, Erto A, Bortone I, et al., Experimental and simulation study of the restoration of a thallium (I)-contaminated aquifer by Permeable Adsorptive Barriers (PABs). Science of The Total Environment, Volume 630, July 2018, pp. 62-71

https://doi.org/10.1016/j.scitotenv.2018.02.169